1 EEG signals index a global signature of arousal embedded in neuronal

population recordings

3

2

4 Richard Johnston^{1, 2, 3}, Adam C. Snyder^{4, 5, 6}, Rachel S. Schibler⁷, and Matthew A. Smith^{1, 2, 3}

5

- 6 ¹Department of Biomedical Engineering, Carnegie Mellon University, Pittsburgh, USA;
- ⁷ Neuroscience Institute, Carnegie Mellon University, Pittsburgh, USA; ³Center for the Neural Basis
- 8 of Cognition, Carnegie Mellon University, Pittsburgh, USA; ⁴Department of Brain and Cognitive
- 9 Sciences, University of Rochester, Rochester, USA; ⁵Department of Neuroscience, University of
- 10 Rochester, Rochester, USA; ⁶Center for Visual Science, University of Rochester, Rochester, USA; ⁷
- 11 Harvey Mudd College, California, USA.

12

- 13 Corresponding author:
- 14 Matthew A. Smith, PhD
- 15 Carnegie Mellon University
- 16 Department of Biomedical Engineering and Neuroscience Institute
- 17 Mellon Institute, Room 115
- 18 Pittsburgh
- 19 Pa, 15213
- 20 Email: mattsmith@cmu.edu

21

- 22 Acknowledgements:
- 23 M.A.S. was supported by NIH Grants R01 EY-029250, R01 MH-118929, R01 EB-026953, and P30
- 24 EY-008098; NSF Grant NCS 1954107; a career development grant and an unrestricted award from
- Research to Prevent Blindness; and the Eye and Ear Foundation of Pittsburgh. A.C.S. was supported
- by NIH grant K99 EY025768. R.S.S. was supported by NIH Grant R90 DA023426. The authors
- would like to thank Ms. Samantha Schmitt for assistance with surgery and data collection.

28

29

<u>Abstract</u>

Electroencephalography (EEG) has long been used to index brain states, from early studies describing activity in the presence and absence of visual stimulation to modern work employing complex perceptual tasks. These studies have shed light on brain-wide signals but often lack explanatory power at the single neuron level. Similarly, single neuron recordings can suffer from an inability to measure brain-wide signals accessible using EEG. Here, we combined these techniques while monkeys performed a change detection task and discovered a novel link between spontaneous EEG activity and a neural signal embedded in the spiking responses of neuronal populations. This "slow drift" was associated with fluctuations in the subjects' arousal levels over time: decreases in pre-stimulus alpha power were accompanied by increases in pupil size and decreases in microsaccade rate. These results show that brain-wide EEG signals can be used to index modes of activity present in single neuron recordings, that in turn reflect global changes in brain state that influence perception and behavior.

Significance Statement

Decades of research has used electroencephalography (EEG) to investigate how voltage fluctuations on the scalp are related to cognition. These studies are useful for measuring brain-wide signals in a non-invasive manner, but they lack the ability to detect small-scale changes at the level of single neurons. In this study, we bridged this gap by recording EEG and spiking responses in the brain while macaques performed a perceptual decision-making task. We found that a commonly used metric of arousal in human EEG studies, pre-stimulus alpha power, is associated with slow drifts in the activity of cortical neurons. Together, these recordings made non-invasively on the scalp and directly in the brain were predictive of changes in arousal levels over time.

Introduction

55

56

57

58

59

60

61

62

63

64

65

66

67

68

69

70

71

72

73

74

75

76

77

78

79

80

For decades, researchers have investigated how the spiking responses of single cortical neurons relate to performance on decision-making (Britten et al., 1996), attention (Moran and Desimone, 1985) and working memory (Fuster and Alexander, 1971) tasks. Interactions between pairs of neurons have also been studied extensively since technological advances in neural recording systems (e.g. microelectrode arrays and two-photon imaging) made it possible to monitor the activity of neural populations simultaneously (Zohary et al., 1994; Cohen and Maunsell, 2009; Leavitt et al., 2017). At the same time, it is becoming increasingly apparent that major insight about the neurobiological basis of cognition can be gained from the study of populations of neurons (Cohen and Maunsell, 2011; Harvey et al., 2012; Mante et al., 2013; Driscoll et al., 2017; Murray et al., 2017; Ni et al., 2018; Remington et al., 2018; Khanna et al., 2019; Oby et al., 2019; Valente et al., 2021). Furthermore, it has been shown that low-dimensional neural activity patterns can be used to index global brain states, which influence performance on cognitive tasks. For example, Stringer et al. (2019) applied principal component analysis (PCA) to data recorded from more than 10,000 neurons in the mouse and found that fluctuations in the first principal component were associated with a host of arousal-related variables including whisking, pupil size, and running speed. Musall et al. (2019) found that uninstructed movements, which themselves may occur at varying frequency based on arousal, were related to brain-wide activity in the mouse. In our own work in rhesus macaques, we have reported a pervasive "slow drift" of neural activity (Cowley et al., 2020), which is correlated with a distinctive pattern of eye metrics that is strongly indicative of changes in arousal (Johnston et al., 2021). However, it is unknown if slow drift is associated with other arousal-related variables that can be measured in a rapid, accurate and non-invasive manner. Spontaneous (i.e., pre-stimulus) oscillations in the alpha frequency band (~8-12Hz) are associated with lateralized changes in spatial attention and global changes in arousal. For example, studies investigating the effects of spatial attention on EEG activity have found that pre-stimulus alpha power is decreased in the visual cortex contralateral to the attended location (Worden et al.,

2000; Sauseng et al., 2005; Kelly et al., 2006; Thut et al., 2006). In contrast, studies exploring the processes underlying perceptual decision-making have uncovered an association between task performance and brain-wide changes in pre-stimulus alpha power. To be more precise, the likelihood of detecting a near threshold visual stimulus increases when pre-stimulus oscillations in the alpha band decrease (Ergenoglu et al., 2004; Babiloni et al., 2006; Hanslmayr et al., 2007; van Dijk et al., 2008; Busch et al., 2009; Mathewson et al., 2009; Romei et al., 2010). Recent work suggests that these global effects (that occur across a range of frontal, midline, and occipital sites) arise due to changes in arousal. According to signal detection theory (Green and Swets, 1966), differences in performance on perceptual decision-making tasks can either reflect shifts in sensitivity or response criterion. Several studies have sought to dissociate these components in macaque monkeys (Luo and Maunsell, 2015, 2018; Crapse et al., 2018; Jun et al., 2021) and similar work has been conducted in human subjects using EEG. For example, it has been shown that brain-wide decreases in pre-stimulus alpha power are associated with increased hit rate and false alarm rate on perceptual decision-making tasks (Limbach and Corballis, 2016; Iemi et al., 2017). These results point to a link between prestimulus alpha power and response criterion, a variable that is modulated, at least in part, by subcortical regions that control arousal levels (de Gee et al., 2017).

One structure that has been implicated in the control of arousal is the locus coeruleus (LC) (Aston-Jones and Cohen, 2005; Sara, 2009; Chandler, 2016). This small region in the pons represents the primary source of norepinephrine to the central nervous system and drives fluctuations in raw and evoked (baseline-corrected) pupil size: non-invasive markers that have been used extensively in the neurosciences to index changes in arousal (Varazzani et al., 2015; Joshi et al., 2016; Reimer et al., 2016; Breton-Provencher and Sur, 2019). Given that the LC is involved in modulating response criterion (de Gee et al., 2017) and pupil size (Joshi and Gold, 2020), one might also expect it to exert an influence on pre-stimulus alpha power. To test this hypothesis non-invasively, one could determine if there is a significant association between pre-stimulus alpha power and pupil size. Several studies have used a combination of EEG and pupillometry to explore if this is the case in humans (Hong et

al., 2014; Van Kempen et al., 2019; Podvalny et al., 2021). For example, Compton et al. (2021) had subjects perform a classic Stroop task and found that alpha power during inter-trial periods was inversely related to raw pupil size. That is, trials with greater pupil size were associated with reduced power in the alpha band and vice versa. These results suggest that spontaneous EEG signals can be used to index global brain state and raise the possibility that they might be associated with other arousal-related metrics such as microsaccade rate.

Microsaccades are small eye movements that occur at a rate of 1-2Hz through the activity of neurons in the superior colliculus (SC) (Rolfs, 2009). As with larger saccades (Burr et al., 1994; Diamond et al., 2000; Knöll et al., 2011), research has shown that visual perception is altered in the hundreds of milliseconds following a microsaccade (Hafed and Krauzlis, 2010; Hafed, 2013; Chen et al., 2015; Chen and Hafed, 2017; Scholes et al., 2018). Interestingly, Bellet et al. (2017) found that these short timescale modulations occur in a rhythmic manner at a frequency of 8–20Hz. However, it is unclear if a relationship exists between alpha oscillations and fixational eye movements at longer timescales, which are more likely to be associated with changes in a subject's internal state (Cowley et al., 2020). Recent work in our laboratory found that slow fluctuations in raw pupil size over the course of a recording session were negatively correlated with microsaccade rate (Johnston et al., 2021). That is, microsaccade rate decreased under conditions of heightened arousal (as indexed by greater pupil size) and vice versa. As described above, the relationship between pre-stimulus alpha power and microsaccade rate has not yet been explored at long timescales. However, based on our previous results, one might expect there to be a positive correlation between these two variables over time.

The primary aim of this study was to determine if EEG signals recorded on the scalp can be used to index a neural measure of brain state acquired directly from the spiking activity of neural populations termed "slow drift". In addition, we investigated if pre-stimulus oscillations in the alpha band are associated with two non-invasive metrics that have previously been used to index global shifts in arousal and that we have found to be related to "slow drift" (Johnston et al., 2021): raw pupil

size and microsaccade rate. EEG from the scalp and spiking activity from populations of neurons in V4 was simultaneously recorded from two monkeys while they performed an orientation-change detection task (Figure 1A). Results showed that fluctuations in pre-stimulus alpha power over the course of a recording session were companied by changes in raw pupil size and microsaccade rate. As expected, pre-stimulus power in the alpha band was negatively correlated with raw pupil size and positively correlated with microsaccade rate. Interestingly, we also found a significant correlation between pre-stimulus alpha power and neural slow drift. This finding is of particular importance as it suggests that spontaneous components of the EEG signal recorded non-invasively on the scalp index low-dimensional patterns of neural activity acquired from microelectrode array recordings in the brain. These results support previous research showing that slow drift is associated with changes in arousal over time (Cowley et al., 2020; Johnston et al., 2021), and provide a strong link between global measurements made across recording modalities and species.

Methods

Subjects

Two adult male rhesus macaque monkeys (*Macaca mulatta*) were used in this study. A previous report (Snyder et al., 2018b) presented analysis of different aspects of the same experiments described here. This study reports the results from a subset of the data from Snyder et al. (2018b) in which EEG was recorded. Surgical procedures to chronically implant a titanium head post (to immobilize the subjects' heads during experiments) and microelectrode arrays were conducted in aseptic conditions under isoflurane anesthesia, as described in detail by Smith and Sommer (2013). Opiate analgesics were used to minimize pain and discomfort during the perioperative period. Neural activity was recorded using 100-channel "Utah" arrays (Blackrock Microsystems) in V4 (Monkey Pe = right hemisphere; Monkey Wa = left hemisphere). The arrays comprised a 10x10 grid of silicon microelectrodes (1 mm in length) spaced 400 μm apart. Experimental procedures were approved by the Institutional Animal Care and Use Committee of the University of Pittsburgh and were performed

in accordance with the United States National Research Council's Guide for the Care and Use of Laboratory Animals.

Microelectrode array recordings

Signals from each microelectrode in the array were amplified and band-pass filtered (0.3–7500Hz) by a Grapevine system (Ripple). Waveform segments crossing a threshold (set as a multiple of the root mean square noise on each channel) were digitized (30KHz) and stored for offline analysis and sorting. First, waveforms were automatically sorted using a competitive mixture decomposition method (Shoham et al., 2003). They were then manually refined using custom time amplitude window discrimination software (code available at https://github.com/smithlabvision/spikesort), which takes into account metrics including (but not limited to) waveform shape and the distribution of interspike intervals (Kelly et al., 2007). A mixture of single and multiunit activity was recorded, but we refer here to all units as "neurons". The mean number of V4 neurons across sessions was 41 (SD = 10) for Monkey Pe and 21 (SD = 10) for Monkey Wa.

EEG recordings

We recorded EEG from 8 Ag/AgCl electrodes (Grass Technologies) adhered to the scalp with electrically conductive paste. The electrodes were positioned roughly at the following locations: Fz, Iz, CP3, CP4, F5, F6, PO7, and PO8 (see Fig. 1B). Signals for each electrode were referenced online to a steel screw on the titanium head post, digitized at 1kHz and amplified by a Grapevine system (Ripple) and low-pass filtered online at 250Hz. They were then rereferenced to the average activity across all electrodes for the entire session. One of the challenges associated with simultaneously recording EEG and the spiking responses of neural populations is the introduction of craniotomies and microelectrode recording arrays. Importantly, previous work in our lab has shown that this does not significantly alter the way current flows to the scalp (Snyder et al., 2018a). We found that FFTs computed before and after craniotomies (performed to implant microelectrode arrays) are highly correlated suggesting that our results are generalizable to EEG recorded from human subjects with an intact skull. Segments of EEG data were recorded for each electrode during the first 300ms of pre-

stimulus periods on the change detection task (Figure 1A). A constant duration was needed in order to remove aperiodic activity that has a 1/f-like distribution (Donoghue et al., 2020). We did not include the first pre-stimulus period due to an increase in eye position variability resulting from fixation having been established a short time earlier. Such variability was not present in the following pre-stimulus periods (see Figure 1 in Johnston et al., 2021). Several outlier rejection steps were then taken. First, segments of EEG data were considered excessively noisy and removed if any of the electrodes had a standard deviation that was 10 times greater than the mean of the entire session, or if any of the electrodes exhibited a flat signal defined as a standard deviation less than 300 nanovolts (Snyder et al., 2018a). Segments of EEG data were also removed if there was evidence of excessive variability in the eye trace. For each session, we computed 1D eye velocity during each pre-stimulus period. EEG segments were removed if the standard deviation of the eye velocity was 2 times greater than the mean eye velocity across all pre-stimulus periods. This final step was necessary to ensure that changes in pre-stimulus alpha power did not arise due to eye movement artifacts.

Visual stimuli

Visual stimuli were generated using a combination of custom software written in MATLAB (The MathWorks) and Psychophysics Toolbox extensions (Brainard, 1997; Pelli, 1997). They were displayed on a CRT monitor (resolution = 1024 X 768 pixels; refresh rate = 100Hz), which was viewed at a distance of 36cm and gamma-corrected to linearize the relationship between input voltage and output luminance using a photometer and look-up-tables.

Behavioral task

Subjects fixated a central point (diameter = 0.6°) on the monitor to initiate a trial (Figure 1A). Each trial comprised a sequence of stimulus periods (400ms) separated by brief pre-stimulus (fixation) periods. The duration of each pre-stimulus period was drawn at random from a uniform distribution spanning 300-500ms but EEG data were only analyzed during the first 300ms (see above). The 400ms stimulus periods comprised pairs of drifting full-contrast Gabor stimuli. One stimulus was presented in the aggregate receptive field (RF) of the recorded V4 neurons, whereas the

other stimulus was presented in the mirror-symmetric location in the opposite hemifield. Although the spatial (Monkey Pe = 0.85cycles/°; Monkey Wa = 0.85cycles/°) and temporal frequencies (Monkey Pe = 8cycles/s; Monkey Wa = 7cycles/s) of the stimuli were not optimized for each individual V4 neuron they did evoke a strong response from the population. The orientation of the stimulus in the aggregate RF was chosen at random to be 45 or 135° , and the stimulus in the opposite hemifield was assigned the other orientation. There was a fixed probability (Monkey Pe = 30%; Monkey Wa = 40%) that one of the Gabors would change orientation by ± 1 , ± 3 , ± 6 , or $\pm 15^\circ$ on each stimulus presentation. The sequence continued until the subject: 1) made a saccade to the changed stimulus within 400ms ("hit"); 2) made a saccade to an unchanged stimulus ("false alarm"); or 3) remained fixating for more than 400ms after a change occurred ("miss"). If the subject correctly detected an orientation change, they received a liquid reward. In contrast, a time-out occurred if the subject made a saccade to an unchanged stimulus delaying the beginning of the next trial by 1s. It is important to note that the effects of spatial attention were also investigated (although not analyzed in this study) by cueing blocks of trials such that the orientation change was 90% more likely to occur in one hemifield relative to the other hemifield.

Eye tracking

Eye position and pupil diameter were recorded monocularly at a rate of 1000Hz using an infrared eye tracker (EyeLink 1000, SR Research).

Microsaccade detection

Microsaccades were defined as eye movements that exceeded a velocity threshold of 6 times the standard deviation of the median velocity for at least 6ms (Engbert and Kliegl, 2003). They were required to be separated in time by at least 100ms. In addition, we removed microsaccades with an amplitude greater than 1° and a velocity greater than 100°/s. To assess the validity of our microsaccade detection method, the correlation (Pearson product-moment correlation coefficient) between the amplitude and peak velocity of detected microsaccades (i.e., the main sequence) was computed for each session. The mean correlation between these two metrics across sessions was 0.84

(SD = 0.06) indicating that our detection algorithm was robust as microsaccades fell on the main sequence (Zuber et al., 1965).

Pre-stimulus power

For each electrode, FFTs were computed using Hanning-windowed segments of EEG data spanning the first 300ms of the pre-stimulus period (Figure 1A). Note that we did not include the first pre-stimulus period due to an increase in eye position variability resulting from fixation having been established a short time earlier (see above). The data for each electrode was then binned using a 30-minute sliding window (step size = 6 minutes), which yielded eight FFTs per time bin (one for each electrode). We wanted to rule out the possibility that slow drift was associated with gradual changes in 1/f noise (Donoghue et al., 2021). Therefore, the aperiodic component of the signal was estimated by fitting an exponential to the binned FFTs for each electrode (Donoghue et al., 2020). Residual power was then computed by subtracting off the aperiodic portion of the signal. Previous research has shown that pre-stimulus alpha power is associated with performance on visual detection tasks across a range of frontal, midline, and posterior electrodes (Ergenoglu et al., 2004; Busch et al., 2009; Iemi et al., 2017). Hence, the aperiodic adjusted (residual) FFTs from all eight electrodes were averaged together for each time bin. Finally, we computed the mean residual power in different frequency bands. For each time bin, residual power was computed in the theta (4-8Hz), alpha (8–12Hz), beta (12–30Hz) and gamma (30–50Hz) bands.

Eye metrics

Mean pupil diameter was measured during stimulus periods, whereas microsaccade rate was measured during pre-stimulus periods (Johnston et al., 2021). We did not include the initial fixation period when measuring microsaccade rate. As described above, there was an increase in eye position variability during this period resulting from fixation having been established a short time earlier (300-500ms). Such variability was not present in following pre-stimulus periods (see Figure 1 in Johnston et al., 2021). Reaction time and saccade velocity were measured on trials in which the subjects were rewarded for correctly detected an orientation change. Reaction time was defined as the time from

when the change occurred to the time at which the saccade exceeded a velocity threshold of 150°/s. Saccade velocity was the peak velocity of the saccade to the changed stimulus. To isolate slow changes in the eye metrics over time, the data for each session was binned using a 30-minute sliding window stepped every 6 minutes. The width of the window, and the step size, were chosen to isolate slow changes over time based on previous research. They were the same as those used by Cowley et al. (2020) and Johnston et al. (2021), which meant direct comparisons could be made across studies.

Calculating slow drift

The spiking responses of populations of neurons in V4 were measured during a 400ms period that began 50ms after stimulus presentation (Figure 1A). Research has shown that neurons in V4 are tuned for stimulus orientation (Desimone and Schein, 1987). To prevent the PCA identifying components related to stimulus tuning, residual spike counts were computed by subtracting the mean response for a given orientation (45 or 135°) across the entire session from individual responses to that orientation. To isolate slow changes in neural activity over time, residual spike counts for each V4 neuron were binned using a 30-minute sliding window stepped every 6 minutes. PCA was then performed to reduce the high-dimensional residual data to a smaller number of latent variables (Cunningham and Yu, 2014). Slow drift in V4 was estimated by projecting the binned residual spike counts for each neuron along the first principal component.

Aligning slow drift across sessions

As described above, slow drift was calculated by projecting binned residual spike counts along the first principal component. The weights in a PCA can be positive or negative (Jolliffe and Cadima, 2016), which meant the sign of the correlation between slow drift and a given metric was arbitrary. Preserving the sign of the correlations was particularly important in this study because we were interested in whether slow drift was associated with a pattern that is indicative of changes in the subjects' arousal levels over time i.e., decreased pre-stimulus alpha power, increased pupil size and decreased microsaccade rate. For simplicity, we adopted an identical approach to that used in our previous study (Johnston et al., 2021). That is, the sign of the slow drift was flipped if the majority of

neurons had negative weights. Forcing the majority of neurons to have positive weights established a common reference frame in which an increase in the value of slow drift was associated with higher firing rates among the majority of neurons.

Estimating the timescale of slow drift and pre-stimulus alpha power

To determine the timescale at which each variable fluctuated over the course of a session Gaussian smoothing was performed (Cowley et al., 2020). The first thing to note is that slow drift was computed in a slightly different manner. To improve temporal resolution, the thirty-minute sliding window (used to bin residual spike counts) was stepped every 1 minute instead of every 6 minutes. The same approach was taken when computing pre-stimulus alpha power. Gaussian smoothing was then performed in a cross-validated manner using standard deviations (i.e., timescales) ranging from 1 to 90 minutes (step size = 1 minute). To determine the timescale of the fluctuation, a R^2 was computed for each standard deviation by leaving out randomly chosen time points for each fold (10 in total) and then predicting the value of each held-out point by calculating a Gaussian weighted average of its neighbors. We found the standard deviation with the maximum R^2 and the standard deviation at which the R^2 dropped to 75% of the maximum R^2 . The latter was taken to be the timescale of the fluctuation.

Choice of analysis time windows

We chose to analyze spiking responses during stimulus periods for consistency across studies. This was the approach taken in our original paper that discovered a slow drift of neural activity in macaque visual and prefrontal cortex (Cowley et al., 2020) and in a follow-up study that included other eye-related metrics such as microsaccade rate and evoked pupil size (Johnston et al., 2021). The reason we chose to analyze microsaccade rate during pre-stimulus periods was to avoid bi-phasic changes that occur during visual stimulus presentation. More specifically, microsaccade rate decreases shortly after a visual stimulus has been presented and then increases later (Engbert and Kliegl, 2003; Rolfs et al., 2008; Hafed and Ignashchenkova, 2013). With regards to segments of EEG data, decades of research has shown that decreased alpha power during pre-stimulus periods is

associated with improved performance on change detection tasks (Ergenoglu et al., 2004; Babiloni et al., 2006; Hanslmayr et al., 2007; van Dijk et al., 2008; Busch et al., 2009; Mathewson et al., 2009; Romei et al., 2010). Therefore, we adopted the same approach and analyzed segments of EEG data during pre-stimulus periods.

Data availability

- All data and code for this manuscript are available at the following link:
- 320 https://doi.org/10.1184/R1/19248827

Results

To determine if spontaneous components of the EEG signal can provide insight into the internal brain state associated with slow drift, we trained two macaque monkeys to perform an orientation-change detection task in which pairs of stimuli were repeatedly presented (Figure 1A). Spiking responses of populations of neurons in visual cortex (V4) were recorded using 100-channel "Utah" arrays as well as EEG on the scalp (Figure 1B). For each electrode, FFTs were computed using segments of EEG data recorded during pre-stimulus periods. The data were then binned using a 30-minute sliding window stepped every 6 minutes (Figure 2A). Prior to averaging across electrodes, aperiodic activity that was 1/f-like in nature was estimated and subtracted off (see *Methods*). Finally, mean residual power was computed in distinct frequency bands. Our primary focus was on pre-stimulus alpha oscillations, but we also computed pre-stimulus power in the theta, beta, and gamma bands. In addition, raw pupil size and microsaccade rate were recorded during stimulus and pre-stimulus periods, respectively.

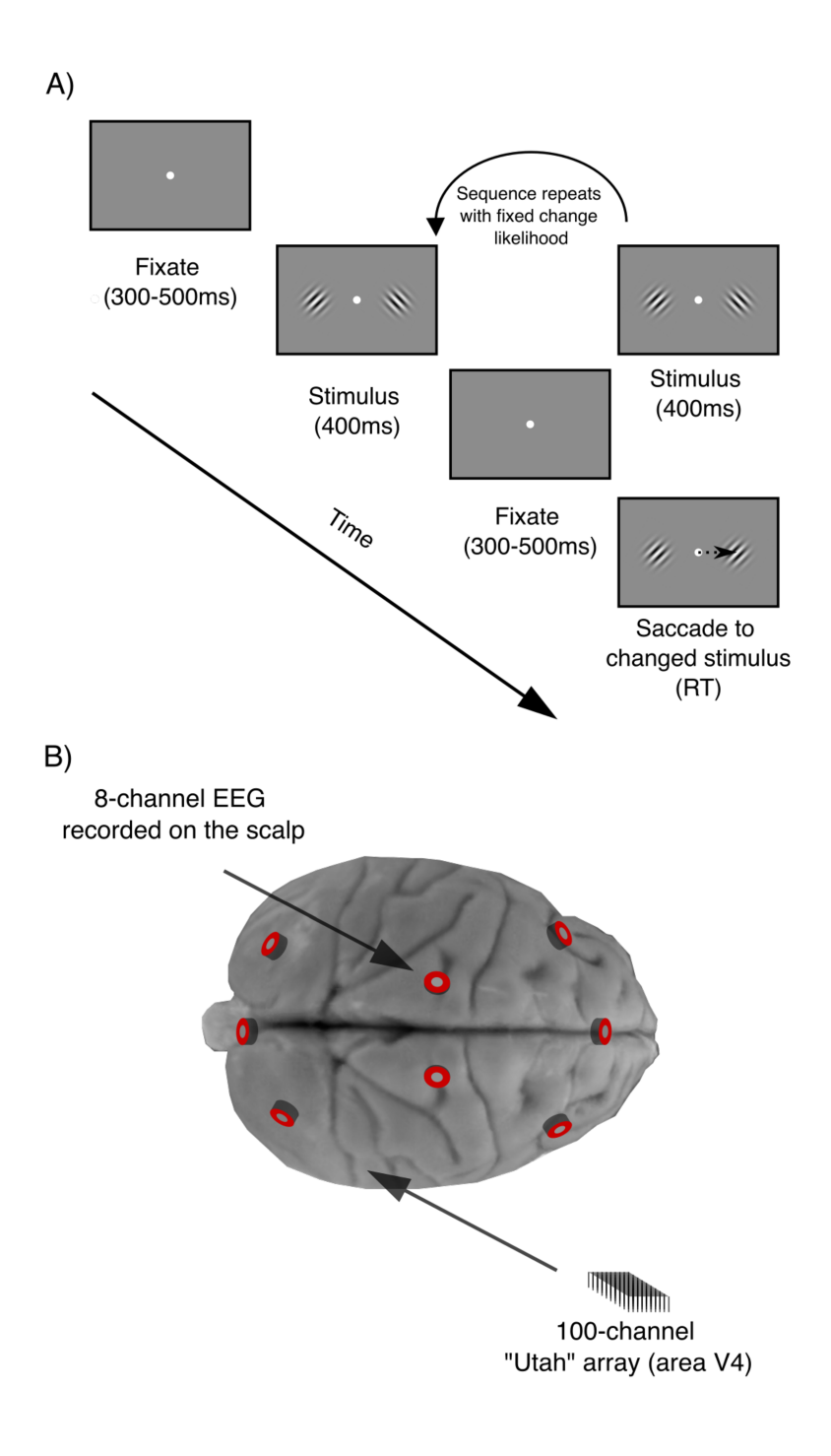


Figure 1. Experimental methods. (A) Orientation-change detection task. After an initial fixation period, a sequence of stimuli (orientated Gabor pairs separated by brief pre-stimulus periods spanning 300-500ms) was presented. The subject's task was to detect an orientation change in one of the stimuli and make a saccade to the changed stimulus. (B) Electrophysiological recordings. We simultaneously recorded: 1) spiking responses of populations of neurons in V4 using 100-channel microelectrode ("Utah") arrays; and 2) EEG from 8 electrodes positioned on the scalp. Spiking responses of populations of neurons in V4 were recorded during 400ms stimulus periods, whereas EEG was recorded during the first 300ms of pre-stimulus periods.

Correlation between pre-stimulus alpha power and raw pupil size

First, we explored the relationship between pre-stimulus alpha power and raw pupil size. As described above, several studies in humans have established a link between these two variables using a combination of EEG and pupillometry (Hong et al., 2014; Van Kempen et al., 2019; Podvalny et al., 2021). Most recently, Compton et al. (2021) found that alpha power during inter-trial periods on a Stroop task was inversely related to raw pupil size. That is, trials with greater pupil size were associated with reduced power in the alpha band and vice versa. To investigate if a similar relationship was found in our data, raw pupil size measurements were binned using the same 30-minute sliding window that was used to bin the EEG data. Note that the width of the window, and the step size, were chosen to isolate slow changes over time based on previous studies we performed (Cowley et al., 2020; Johnston et al., 2021). Example sessions for Monkey Pe and Monkey Wa are shown in Figure 2B (top and bottom rows, respectively). In support of previous research, pre-stimulus power in the alpha band was negatively associated with raw pupil size in each example session for both subjects.

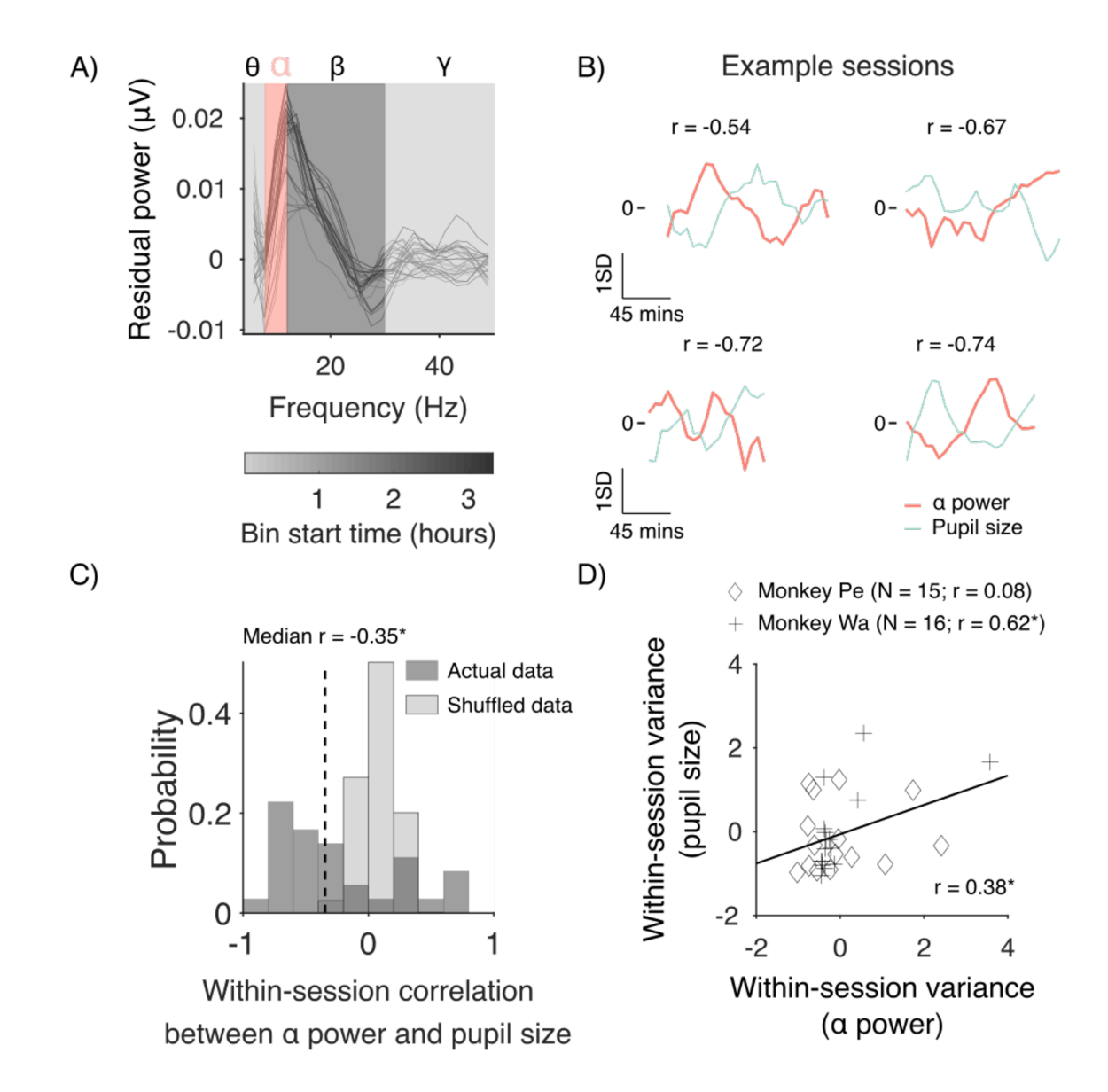


Figure 2. Correlation between pre-stimulus alpha power and raw pupil size. (A) Isolating slow fluctuations in pre-stimulus alpha power. A mean FFT was computed for each large 30-minute bin (represented by gray lines) by averaging across electrodes. Note that the aperiodic portion of the signal was removed prior to averaging across electrodes (see Methods), which explains why residual power, as opposed to raw power, is shown on the y-axis. (B) Four example sessions in which there was a moderate to strong correlation between pre-stimulus alpha power and raw pupil size. The top row contains two sessions for Monkey Pe, whereas the bottom row contains two sessions for Monkey Wa. Note that the data were zscored for visualization purposes only (i.e., so that variables with different units could be shown on the same plot). (C) A histogram showing the distribution of correlation values across sessions between pre-stimulus alpha power and raw pupil size. We used a Wilcoxon signed rank test to test the null hypothesis that the median correlation across sessions was equal to zero (Monkey Pe: median r = -0.41, p = 0.008; Monkey Wa: median r = -0.31, p = 0.301). (D) A scatter plot showing how the magnitude of fluctuations in pre-stimulus alpha power (as measured by computing within-session variance) relate to the magnitude of fluctuations in raw pupil size. Note that the data were z-scored separately for each Monkey to control for potential differences in variance between subjects. Failing to control for this might have led to an artifactual correlation if the variance for one subject was greater than the other or vice versa. Individual correlations for each monkey have been reported in the figure legend along with the number of sessions included in the analysis. SD = standard deviation. θ = theta, $\alpha = \text{alpha}$, $\beta = \text{beta}$, $\gamma = \text{gamma}$. $p < 0.05^*$, $p < 0.01^{**}$, $p < 0.001^{***}$.

375

376

377

378

379

380

381

382

383

384

385

386

387

388

389

390

393

394

395

396

397

398

399

400

401

402

403

404

405

406

407

408

409

410

411

412

413

414

415

416

417

The example sessions in Figure 2B exhibit moderate to strong trends. However, it is difficult to determine if two variables that fluctuate slowly over time are correlated over the course of a single session. Standard correlation analyses assume that all samples are independent, but smoothed variables can violate this assumption leading to "nonsense" correlations" between variables that are unrelated (Harris, 2020). An easy way to overcome this problem is to record data from multiple sessions. Two approaches can then be adopted: 1) one can compute a correlation for each session, and then perform a statistical test to investigate if the distribution of coefficients across sessions is centered on zero; or 2) one can explore if the magnitude of fluctuations in one of the variables is associated with the magnitude of fluctuations in the other variable. Both approaches were adopted in the present study to investigate if there was a relationship between pre-stimulus alpha power and pupil size across sessions (Monkey Pe = 15 sessions; Monkey Wa = 16 sessions). First, we investigated if pre-stimulus power in the alpha band and raw pupil size were correlated over time. Within each session, we computed a correlation (Pearson product-moment correlation coefficient) between prestimulus alpha power and raw pupil size. As in our previous study (Johnston et al., 2021), we found that null distributions (generated by computing correlations between sessions recorded on different days) were centered on zero. Therefore, a Wilcoxon signed rank test was then used to test the null hypothesis that the median correlation across sessions was equal to zero. Consistent with the pattern of results observed in the four example sessions, we found that pre-stimulus alpha power was significantly and negatively correlated with raw pupil size (Figure 2C, median r = -0.35, p = 0.012). Next, we investigated if the magnitude of changes in EEG alpha power was correlated with the magnitude of changes in raw pupil size. Within each session, we computed the variance of prestimulus alpha power and raw pupil size. The data were then z-scored for each monkey separately to control for potential differences in variance that might have led to an artifactual correlation when the data were pooled across subjects. Finally, a correlation (Pearson product-moment correlation coefficient) was performed to investigate if within-session variance in pre-stimulus alpha power was

significantly associated with within-session variance in raw pupil size. Results showed that the magnitude of changes in pre-stimulus alpha power was significantly correlated with the magnitude of changes in raw pupil size (Figure 2D, r = 0.38, p = 0.035). These findings support previous work in humans as they show that fluctuations in pre-stimulus alpha power were accompanied by global changes in the subjects' arousal levels (Hong et al., 2014; Van Kempen et al., 2019; Compton et al., 2021; Podvalny et al., 2021). This motivated us to ask if pre-stimulus alpha power is associated with other arousal-related metrics such as microsaccade rate.

Correlation between pre-stimulus alpha power and microsaccade rate

Recently, we found that microsaccade rate fluctuates over the course of a recording session in a manner that is consistent with slow changes in arousal over time (Johnston et al., 2021). More specifically, decreases in raw pupil size on a change detection task were accompanied by increases in microsaccade rate and vice versa. Hence, we were interested in whether pre-stimulus alpha power is correlated with microsaccade rate. Based on our previous research, we hypothesized that microsaccade rate would be positively correlated with pre-stimulus alpha power. To test this prediction, microsaccade rate measurements were binned using the same 30-minute sliding window stepped every 6 minutes. Example sessions for Monkey Pe and Monkey Wa are shown in Figure 3A (top and bottom rows, respectively). In support of our hypothesis, pre-stimulus alpha power was positively associated with microsaccade rate in each example session for both subjects.

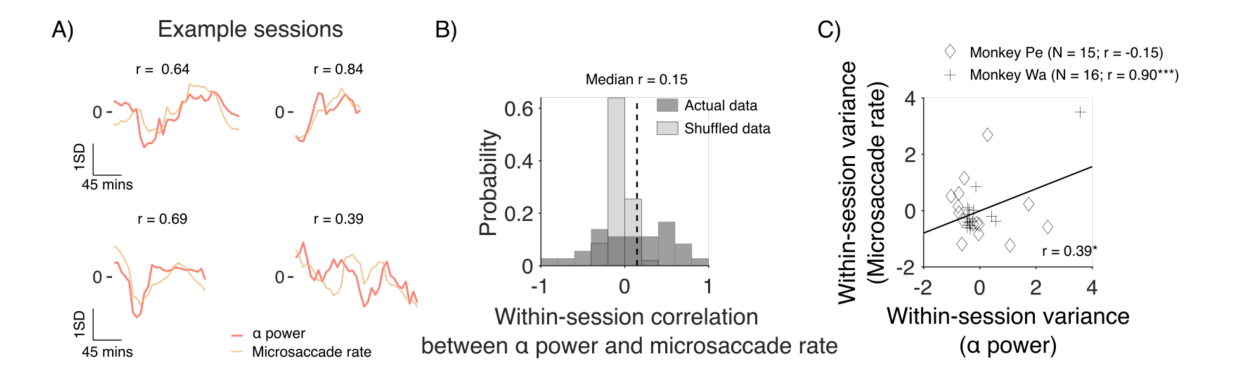


Figure 3. Correlation between pre-stimulus alpha power and microsaccade rate. (A) Four example sessions in which there was a moderate to strong correlation between pre-stimulus alpha power and microsaccade rate. The top row contains two sessions for Monkey Pe, whereas the bottom row contains two sessions for Monkey Wa. Note that the data were z-scored for visualization purposes only (i.e., so that variables with different units could be shown on the same plot). (B) A histogram showing the distribution of correlation values across sessions between pre-stimulus alpha power and microsaccade rate. A Wilcoxon signed rank test was used to test the null hypothesis that the median correlation across sessions was equal to zero (Monkey Pe: median r = 0.23, p = 0.008; Monkey Wa: median r = -0.21, p = 0.44). (C) A scatter plot showing how the magnitude of fluctuations in pre-stimulus alpha power (as measured by computing within-session variance) relate to the magnitude of fluctuations in microsaccade rate. Note that the data were z-scored separately for each Monkey to control for potential differences in variance that might have resulted in an artifactual correlation. Individual correlations for each monkey have been reported in the figure legend along with the number of sessions included in the analysis. SD = standard deviation. $\alpha = 1$ alpha. $\alpha = 1$ alpha.

Next, we explored if a similar pattern was present across all sessions (Monkey Pe = 15 sessions; Monkey Wa = 16 sessions). As before, we first investigated if changes in pre-stimulus alpha power and microsaccade rate were correlated over time. Within each session, we computed the correlation (Pearson product-moment correlation coefficient) between pre-stimulus power in the alpha band and microsaccade rate. A Wilcoxon signed rank test was then used to test the null hypothesis that the median correlation across sessions was equal to zero. Despite the compelling trends on some example sessions (Figure 3A), there was no statistically significant correlation between pre-stimulus alpha power and microsaccade rate (Figure 3B, median r = 0.15, p = 0.210). Next, we investigated if the magnitude of changes in pre-stimulus alpha power was correlated with the magnitude of changes in microsaccade rate. Within each session, we computed the variance of pre-stimulus alpha power and microsaccade rate. A correlation (Pearson product-moment correlation coefficient) was then performed on z-scored data to investigate the relationship between within-

Results showed that the magnitude of changes in pre-stimulus alpha power was significantly correlated with the magnitude of changes in microsaccade rate (Figure 3C, r = 0.39, p = 0.029). Although we note that the median within-session correlation between slow drift and microsaccade rate was not significantly different from zero (Figure 3B), the compelling match in the time course of individual sessions (Figure 3A) and the significant session-by-session correlation in variance (Figure 3C) are important for at least two reasons. Firstly, they establish a novel link between pre-stimulus alpha power and fixational eye movements at long timescales. Secondly, they provide further evidence to suggest that fluctuations in pre-stimulus alpha power are associated with changes in arousal. If this is the case, one might expect alpha oscillations to be correlated with behavioral performance and other eye metrics that have been used to index changes in brain state such as saccadic reaction time and saccade velocity (Castellote et al., 2007; Di Stasi et al., 2013; DiGirolamo et al., 2016).

Correlation between pre-stimulus alpha power and other arousal-related metrics

Previously, we found that performance on a change detection task, as measured by computing hit rate and false alarm rate, fluctuates slowly over the course of a recording session (Cowley et al., 2020). The same is also true of other eye metrics including saccadic reaction time and saccade velocity (Johnston et al., 2021). To explore if pre-stimulus alpha power is associated with these additional arousal-related metrics, correlations (Pearson product-moment correlation coefficient) were computed within each session. Wilcoxon signed rank tests were then used to test the null hypothesis that the median correlation across sessions was equal to zero. Results showed that prestimulus alpha power was negatively correlated with false alarm rate (Figure 4, median r = -0.28, p = 0.046). However, it was not significantly correlated with hit rate (Figure 4, median r = 0.03, p = 0.906), reaction time (median r = 0.12, p = 0.176) or saccade velocity (Figure 4, median r = -0.12, p = 0.389). Note that pupil size and microsaccade rate have also been included in Figure 4 so that comparisons can be made across the different behavioral and eye metrics. This data is the same as

that reported in Figure 2C and Figure 3B, respectively. These findings are interesting because they demonstrate that pre-stimulus alpha power is associated with slow fluctuations in behavior over time. Previous research in humans has shown that pre-stimulus oscillations in the alpha band are associated with hit rate and false alarm rate (Iemi et al., 2017). However, it is difficult to make comparisons across studies due to task differences. In our paradigm, subjects had to make a saccade to the changed stimulus, whereas in Iemi et al. (2017) they had to make a yes/no decision about whether a near-threshold stimulus was presented. Either way, our results point to a link between alpha oscillations and global changes in arousal. Next, we asked if pre-stimulus alpha power, a non-invasive signal recorded on the scalp, can be used to index a neural measure of brain state acquired directly from the spiking activity of neural populations.



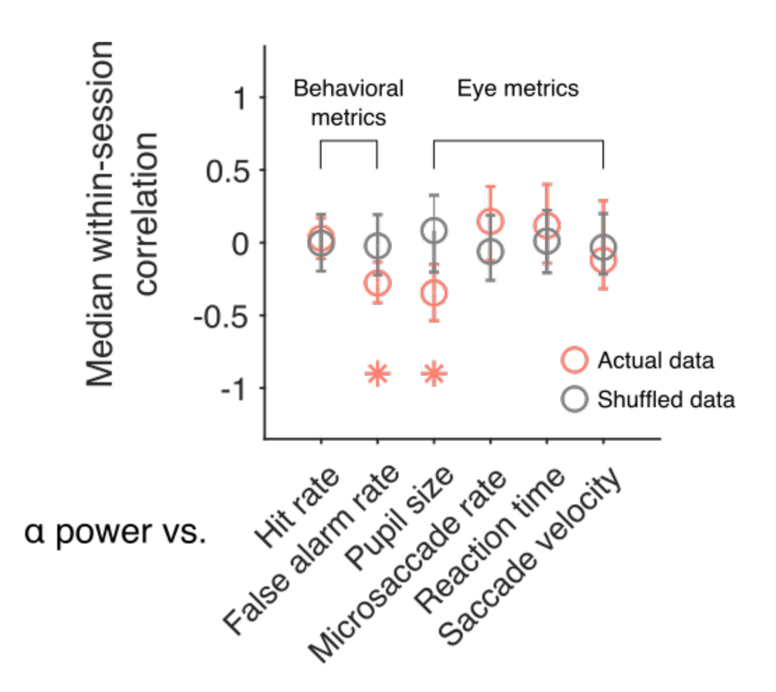


Figure 4. Correlation between slow drift and other arousal-related metrics. A scatter plot showing the median within-session correlation between pre-stimulus alpha power and a host of behavioral and eye metrics analyzed in our previous work (Cowley et al., 2020; Johnston et al., 2021). Note that pupil size and microsaccade rate have also been included so that comparisons can be made across the different behavioral and eye metrics. This data is the same as that reported in Figure 2C and Figure 3B, respectively. For Monkey Pe, the median correlation between α power and false alarm rate was -0.28 (p = 0.083), whereas the median correlation between α power and pupil size was -0.41 (p = 0.008). For Monkey Wa, the median correlation between α power and false alarm rate was -0.24 (p = 0.326), whereas the median correlation

between α power and pupil size was -0.31 (p = 0.301). Error bars represent bootstrapped 95% confidence intervals. α = alpha. p < 0.05*.

Correlation between pre-stimulus alpha power and slow drift

As described above, we recently observed a pervasive signal in visual and prefrontal cortex termed "slow drift" (Cowley et al., 2020). Interestingly, this neural signature was related to a subject's tendency to make impulsive decisions on a change detection task and a constellation of eye metrics that are indicative of slow changes in arousal over time (Johnston et al., 2021). For example, we found that slow drift was positively correlated with raw pupil size and negatively correlated with microsaccade rate. This motivated us to ask if non-invasive EEG signals recorded on the scalp are associated with slow drift. Based on our previous work, we hypothesized that pre-stimulus alpha power would be negatively correlated with slow drift.

To calculate slow drift, residual spike counts were computed by subtracting the mean response for a given orientation across the entire session from individual responses. This was an important first step as it ensured that signals related to stimulus tuning were not present in the slow drift. Residual spike counts were then binned using the same 30-minute sliding window that had been used to bin the EEG, pupil and microsaccade rate data (Figure 5A, see *Methods*). We then applied principal component analysis (PCA) to the neural data and estimated slow drift by projecting the binned residual spike counts along the first principal component (i.e., the loading vector that explained the most variance in the data). The sign of the weights in PCA is arbitrary meaning that the correlation between slow drift and pre-stimulus alpha power in any session was equally likely to be positive or negative (Jolliffe and Cadima, 2016). To overcome this issue, we flipped the sign of the slow drift such that the majority of neurons had positive weights (Hennig et al., 2021). This established a common reference frame in which an increase in the value of the drift was associated with higher firing rates among the majority of neurons (see *Methods*).

We computed the slow drift of the neuronal population in each session using the abovementioned method, and then compared it to pre-stimulus alpha power. Example sessions for Monkey Pe and Monkey Wa are shown in Figure 5B (top and bottom rows, respectively). In support of our hypothesis, pre-stimulus alpha power was negatively correlated with slow drift in each example session for both subjects.

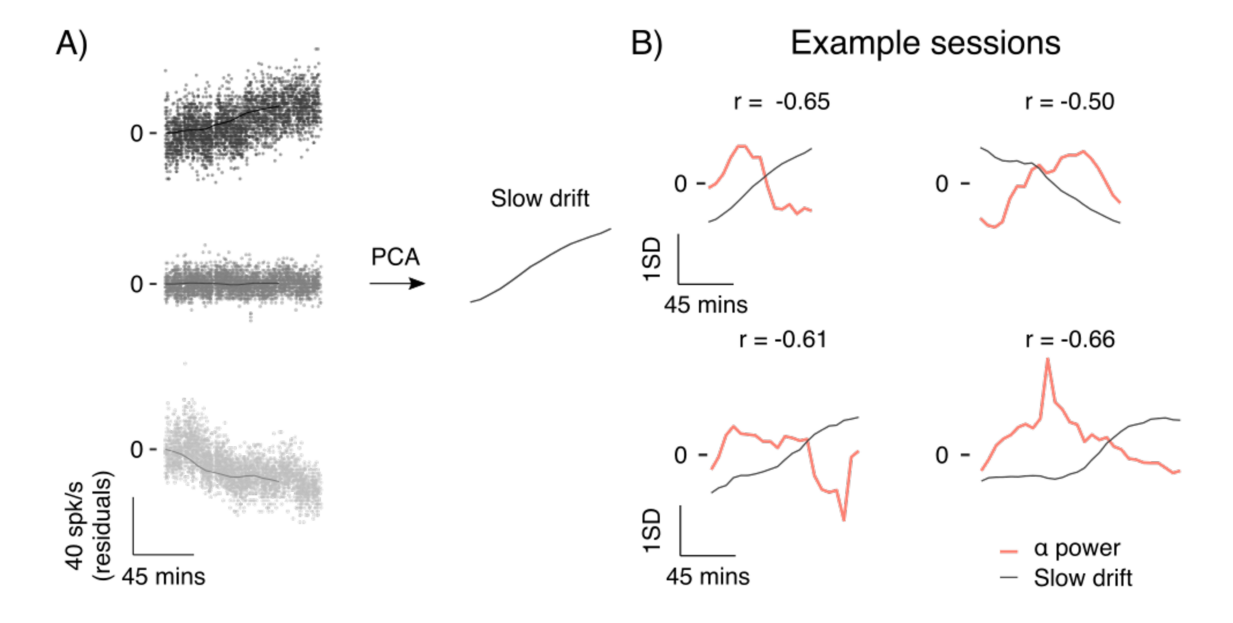


Figure 5. Computing slow drift. (A) Three example neurons recorded during the top left-hand session in (B). Each point represents the mean residual spike count during a 400ms stimulus period. The data were then binned using a 30-minute sliding window stepped every 6 minutes (solid line). PCA was used to reduce the dimensionality of the data and slow drift was computed by projecting binned residual spike counts along the first principal component. (B) Four example sessions in which there was a moderate to strong correlation between pre-stimulus alpha power and slow drift. The top row contains two sessions for Monkey Pe, whereas the bottom row contains two sessions for Monkey Wa. Note that the data were z-scored for visualization purposes only (i.e., so that variables with different units could be shown on the same plot). PCA = Principal Component Analysis. SD = standard deviation. α = alpha.

Next, we explored if a similar pattern was present across sessions (Monkey Pe = 15 sessions; Monkey Pe = 15 sessions). Within each session, a correlation (Pearson product-moment correlation coefficient) was computed between pre-stimulus alpha power and slow drift. Note that correlations were also performed to investigate the relationship between slow drift and pre-stimulus power in the theta, beta, and gamma bands. Wilcoxon signed rank tests were then used to test the null hypothesis that the median correlation across sessions was equal to zero. Consistent with the pattern observed in the example sessions, pre-stimulus power in the alpha band was negatively correlated with slow drift (Figure 6B, median Pe = 0.34, Pe = 0.017). No significant correlation was found between slow drift and

pre-stimulus power in the theta (Figure 6A, median r = -0.03, p = 0.318), beta (Figure 6C, median r = 0.05, p = 0.570) and gamma bands (Figure 6D, median r = 0.11, p = 0.531). These findings suggest that spontaneous components of the EEG signal, namely pre-stimulus alpha power, recorded non-invasively on the scalp can be used to index low-dimensional patterns of neural activity acquired directly in the brain.



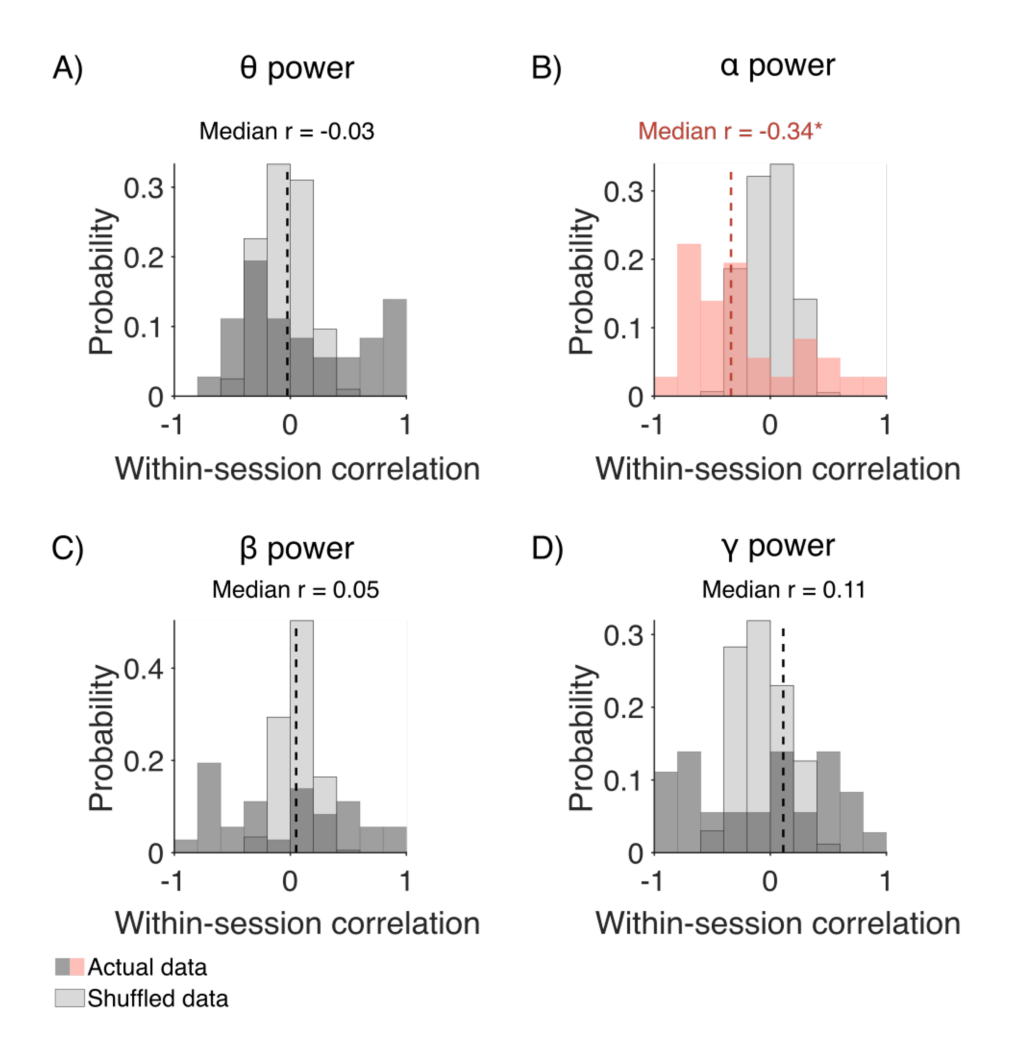


Figure 6. Correlation between slow drift and pre-stimulus power in distinct frequency bands (A-D) Histograms showing distributions of correlation values across sessions. Wilcoxon signed rank tests were used to test the null hypothesis that the median correlation across sessions was equal to zero. The median correlation between slow drift and α power for Monkey Pe was -0.47 (p = 0.041). For Monkey Wa, the median correlation between slow drift and α power was -0.24 (p = 0.215). θ = theta, α = alpha, β = beta, γ = gamma. p < 0.05*, p < 0.01***, p < 0.001***.

The frequency bands in the analysis described above (Figure 6) were chosen based on previous research that has explored the relationship between EEG on the scalp and spiking responses recorded

directly in the brain (Musall et al., 2014; Snyder et al., 2015). However, there are disadvantages to assessing power in pre-defined regions of the power spectrum such as variability in the peak central frequency that is known to be associated with different task demands and/or cognitive states (Mierau et al., 2017). Given our interest in the link between pre-stimulus oscillations and arousal, we performed an additional analysis to investigate if slow drift was associated with power across a wide range of frequencies. To do this, we computed the median within-session correlation between slow drift and pre-stimulus alpha power using a 4Hz sliding window stepped every 2Hz. In support of the analysis described above (Figure 6), which was performed using pre-defined frequency bands, we found that slow drift was only significantly correlated with pre-stimulus power at 8-12Hz, the canonical alpha frequency band (Figure 7, median r = -0.34, p = 0.017).

Correlation between slow drift and pre-stimulus power

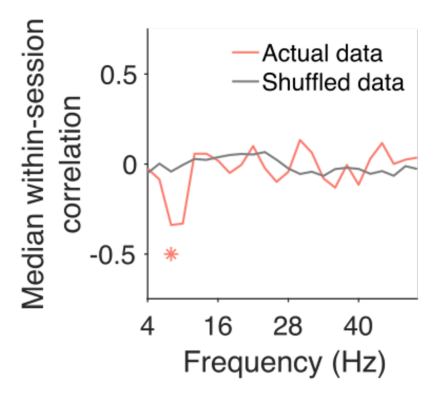


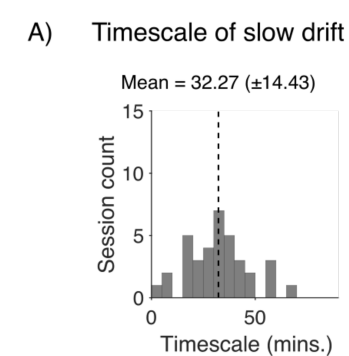
Figure 7. Correlation between slow drift and pre-stimulus power across frequencies. The median within-session correlation was computed using a 4Hz sliding window stepped every 2Hz. Values on the x-axis represent the left edge of the window. The only significant correlation was between slow drift and pre-stimulus power at 8-12Hz i.e., the alpha frequency band (p = 0.017). Note that the p-value for the correlation between slow drift and pre-stimulus power at 10-14Hz was 0.06. p < 0.05*.

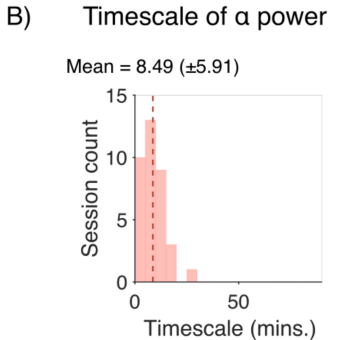
Correlation between the timescale of slow drift and pre-stimulus alpha power

Finally, we investigated if the timescale of slow drift is correlated with the timescale of fluctuations in pre-stimulus alpha power. Note that these two variables are unlikely to have the same timescale because oscillations in the 8 to 12Hz frequency band are influenced by cognitive processes

such as attention that operate at a timescale of hundreds of milliseconds to seconds (Worden et al., 2000; Sauseng et al., 2005; Kelly et al., 2006; Snyder and Foxe, 2010). However, they may be modulated by a joint and continuously graded process (perhaps arising due to fluctuating levels of neuromodulators) that operates at a brain-wide level. If this is the case, one would expect a positive correlation between the timescale of slow drift and the timescale of fluctuations in pre-stimulus alpha power. To determine the optimal timescale at which a variable fluctuated over the course of a session, we used a cross-validated kernel regression method that applied Gaussian smoothing (with standard deviations ranging from 1 to 90 minutes) to the data and returned the time scale for smoothing that best fit held-out data (see *Methods*). We found that the timescale of slow drift (Figure 8A, M = 32.27, SD = 14.43) was significantly longer than the timescale of fluctuations in pre-stimulus alpha power (Figure 8B, M = 9.32, SD = 5.89) (t(65) = 8.28, p < 0.001). However, there was a significant correlation between the timescale of slow drift and pre-stimulus alpha power (r = 0.40, p = 0.0255) from session to session. This suggests that slow drift and pre-stimulus alpha power arise from distinct mechanisms on a moment-by-moment basis but may be linked to, or modulated by, a joint process that drives global changes in arousal over time.







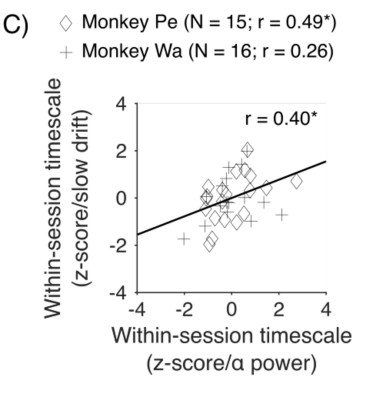


Figure 8. Correlation between the timescale of slow drift and pre-stimulus alpha power (A) A histogram showing the distribution of timescales computed for slow drift across sessions. (B) Same as (A) but for pre-stimulus alpha power. (C) A scatter plot showing how the timescale of slow drift relates to the timescale of fluctuations in pre-stimulus alpha power. Note that the data were z-scored separately for each monkey to control for potential timescale differences between subjects. Failing to control for this might have led to an artifactual correlation if timescales for one subject were greater than those for the other or vice versa. α = alpha. p < 0.05*, p < 0.01***, p < 0.001****.

Discussion

In this study, we investigated if pre-stimulus oscillations in the alpha band could be utilized as an external signature of an internal brain state, a recently discovered neural activity pattern called "slow drift" (Cowley et al., 2020). We know from previous work that slow drift in macaque visual and prefrontal cortex is correlated with a host of eye metrics across tasks with differing cognitive demands (Johnston et al., 2021), suggesting that slow drift can be used to index brain-wide changes in arousal. Since pre-stimulus alpha power is also related to arousal, we wondered if a link could be established between a neural measure of an internal brain state acquired directly from the spiking activity of populations of neurons (i.e., slow drift) and indirect signals recorded non-invasively from the scalp using EEG. Results showed that slow drift was significantly associated with a pattern that is indicative of changes in the subjects' arousal levels over time: decreases in pre-stimulus alpha power were accompanied by increases in raw pupil size and decreases in microsaccade rate.

Several studies in humans have found a relationship between pre-stimulus alpha power and pupil size (Hong et al., 2014; Van Kempen et al., 2019; Podvalny et al., 2021). For example, on classic Stroop tasks, trials with greater raw pupil size are associated with reduced alpha power and vice versa (Compton et al., 2021). Our results support this finding as slow changes in pre-stimulus alpha power were negatively correlated with raw pupil size. Furthermore, there was an association between the magnitude of fluctuations in pre-stimulus alpha power (as measured by computing within-session variance) and the magnitude of fluctuations in raw pupil size. These findings suggest that pre-stimulus alpha power is associated with global changes in brain state that occur naturally over time, perhaps due to fluctuating levels of neuromodulators in the brain. Testing this hypothesis would require the simultaneous recording of EEG from the scalp and spiking activity in subcortical regions associated with arousal such as the LC (Aston-Jones and Cohen, 2005; Sara, 2009; Chandler, 2016). Such studies have been conducted in monkeys (Foote et al., 1980; Swick et al., 1994) but the relationship between pre-stimulus alpha power and pupil size has not been elucidated in awake behaving animals

performing cognitively demanding tasks. Hence, an important question for future research would be to determine how the spiking activity of subcortical regions associated with arousal relates to prestimulus alpha power recorded on the scalp.

653

654

655

656

657

658

659

660

661

662

663

664

665

666

667

668

669

670

671

672

673

674

675

676

677

678

Another non-invasive metric that has been linked to oscillations in the alpha band is microsaccade rate. We know from previous research that visual perception is altered up to 700ms after a microsaccade has occurred, at a frequency of ~8 to 20Hz (Bellet et al., 2017). The results of the present study show that a relationship also exists between alpha oscillations and microsaccade rate at longer timescales. Recently, we found that slow fluctuations in raw pupil size were negatively correlated with microsaccade rate (Johnston et al., 2021). That is, microsaccade rate decreased under conditions of heightened arousal (as indexed by greater pupil size and increased saccade velocity) and vice versa. Given this result, we hypothesized that there would be a positive correlation between pre-stimulus alpha power and microsaccade rate at longer timescales, which are more likely to reflect changes in a subject's internal cognitive state (Cowley et al., 2020). This is exactly what was found in several example sessions for both monkeys. Furthermore, the magnitude of fluctuations in prestimulus alpha power was significantly correlated with the magnitude of fluctuations in microsaccade rate across sessions. A key goal for future research is to bridge the gap between microsaccade-related EEG signals and neural activity in brain regions that have been implicated in eye movement control such as the SC (Martinez-Conde et al., 2013). Research combining EEG and eye tracking has shown that microsaccades are accompanied by: 1) a large potential over occipital electrodes ~100ms after movement onset; and 2) changes in alpha/theta power (Dimigen et al., 2009). However, it is unclear how these signals recorded on the scalp, at relatively short timescales, relate to the activity of SC neurons. Similarly, we do not know how long timescale changes in pre-stimulus alpha power, which we found to be correlated with microsaccade rate, link to firing rates in the SC. Future research combining eye tracking, EEG and single unit/population recordings in the SC is needed to determine the neural underpinnings of non-invasive scalp signals that are associated with fixational eye movements.

Taken together, the results of the pupil size and microsaccade rate analysis suggest that fluctuations in pre-stimulus alpha power are associated with global changes in arousal. This motivated us to ask if non-invasive signals recorded on the scalp can be used to index a recently discovered signature of an internal brain state called "slow drift" (Cowley et al., 2020). We know from previous research that slow drift is positively correlated with raw pupil size and negatively correlated with microsaccade rate across tasks with differing cognitive demands (Johnston et al., 2021). Therefore, we predicted that there would be an inverse relationship between changes in pre-stimulus alpha power and slow drift over time. In support of this hypothesis, we found that slow drift in visual cortex was negatively correlated with pre-stimulus alpha power in several example sessions for both monkeys. Furthermore, they were significantly and negatively correlated when the data were pooled across sessions. It is important to note that this finding cannot be attributed to changes in 1/f noise that are characteristic of several brain disorders (Peterson et al., 2017; Robertson et al., 2019) and healthy ageing (Voytek et al., 2015). Firstly, aperiodic components of the FFT were estimated and subtracted off prior to averaging across electrodes (Donoghue et al., 2020). Secondly, no significant correlation was found between slow drift and pre-stimulus power in the theta, beta, and gamma bands. One might have expected this to be the case if slow drift was associated with uniform shifts in power across frequencies. Nonetheless, 1/f noise and other aperiodic fluctuations, might be related to global brain modulations in ways that are not well captured by the slow drift we observe. A further interesting question is whether slow drift is associated with other EEG signals such as the P1 component of the visually evoked potential (VEP). There are at least two reasons why this might be the case. Firstly, evidence suggests that early VEP components are negatively correlated with pre-stimulus alpha power (Roberts et al., 2014; Iemi et al., 2019). Secondly, decades of research has shown that P1 amplitude is associated with global changes in brain state (Luck et al., 2000). For example, it is significantly larger on trials in which a weak visual stimulus is detected (Ergenoglu et al., 2004; Pourtois et al., 2006; Del Cul et al., 2007; Mathewson et al., 2009) and negatively correlated with reaction time on spatial attention tasks (Mangun and Hillyard, 1991).

679

680

681

682

683

684

685

686

687

688

689

690

691

692

693

694

695

696

697

698

699

700

701

702

703

Another key finding from the present study is related to the timescale of slow drift and fluctuations in pre-stimulus alpha power. We found that the timescale of these two variables was significantly different: pre-stimulus alpha power had a shorter timescale than slow drift. This result is unsurprising given that oscillations in the 8 to 12Hz frequency band are influenced by processes such as attention that operate at a timescale of hundreds of milliseconds to seconds (Worden et al., 2000; Sauseng et al., 2005; Kelly et al., 2006; Snyder and Foxe, 2010). However, we did find that the timescale of slow drift and the timescale of fluctuations in pre-stimulus alpha power was significantly correlated across sessions. This observation is important because it suggests that these two variables are modulated by a common process such as arousal that operates at a brain-wide level. In the present study, there was no experimental manipulation of the subjects' arousal levels meaning that the timescale of slow drift and pre-stimulus alpha power varied naturally from session to session. Evidence suggests that LC is a major source of fluctuations in arousal (Aston-Jones and Cohen, 2005; Sara, 2009; Chandler, 2016). Therefore, activating neurons in this region directly via electrical microstimulation, or indirectly via pharmacological manipulations, should lead to correlated changes in the timescale of slow drift and pre-stimulus alpha power.

In summary, we found that a commonly used metric of cognitive state in human EEG studies, pre-stimulus alpha power, is associated with gradual shifts in the underlying population structure of neural activity throughout the brain. Together, these measures at the scalp, and in the cortex, were predictive of changes in the monkeys' arousal levels over time. These findings show that indirect measures of neural activity can be used to index a global signature of arousal. By linking a vast EEG literature in humans with simultaneous scalp/microelectrode array recordings in macaques our results bridge the gap between large-scale field potentials and the spiking responses of populations of cortical neurons.

References

- Aston-Jones G, Cohen JD (2005) AN INTEGRATIVE THEORY OF LOCUS COERULEUS-
 - NOREPINEPHRINE FUNCTION: Adaptive Gain and Optimal Performance. Annu Rev

- 732 Neurosci 28:403-450. 733 Babiloni C, Vecchio F, Bultrini A, Romani GL, Rossini PM (2006) Pre- and poststimulus alpha 734 rhythms are related to conscious visual perception: A high-resolution EEG study. Cereb Cortex 735 16:1690-1700. 736 Bellet J, Chen CY, Hafed ZM (2017) Sequential hemifield gating of α-and β-behavioral 737 performance oscillations after microsaccades. J Neurophysiol 118:2789–2805. 738 Brainard DH (1997) The Psychophysics Toolbox. Spat Vis 10:433–436 Available at: 739 http://www.ncbi.nlm.nih.gov/pubmed/9176952. Breton-Provencher V, Sur M (2019) Active control of arousal by a locus coeruleus GABAergic 740 741 circuit. Nat Neurosci 22:218–228 Available at: 742 http://www.ncbi.nlm.nih.gov/pubmed/30643295. 743 Britten KH, Newsome WT, Shadlen MN, Celebrini S, Movshon JA (1996) A relationship between 744 behavioral choice and the visual responses of neurons in macaque MT. Vis Neurosci 13:87– 745 100. 746 Burr DC, Morrone MC, Ross J (1994) Selective suppression of the magnocellular visual pathway 747 during saccadic eye movements. Nature 371:511–513 Available at: http://www.ncbi.nlm.nih.gov/pubmed/7935763. 748 749 Busch NA, Dubois J, VanRullen R (2009) The phase of ongoing EEG oscillations predicts visual 750 perception. J Neurosci 29:7869-7876. 751 Castellote JM, Kumru H, Queralt A, Valls-Solé J (2007) A startle speeds up the execution of externally guided saccades. Exp Brain Res 177:129-136. 752
- Chandler DJ (2016) Evidence for a specialized role of the locus coeruleus noradrenergic system in cortical circuitries and behavioral operations. Brain Res 1641:197–206 Available at:

 http://dx.doi.org/10.1016/j.brainres.2015.11.022.
- Chen C-Y, Ignashchenkova A, Thier P, Hafed ZM (2015) Neuronal Response Gain Enhancement
 prior to Microsaccades. Curr Biol 25:2065–2074 Available at:

- 758 http://dx.doi.org/10.1016/j.cub.2015.06.022. 759 Chen CY, Hafed ZM (2017) A neural locus for spatial-frequency specific saccadic suppression in 760 visual-motor neurons of the primate superior colliculus. J Neurophysiol 117:1657–1673. 761 Cohen MR, Maunsell JHR (2009) Attention improves performance primarily by reducing 762 interneuronal correlations. Nat Neurosci 12:1594–1600 Available at: 763 http://www.ncbi.nlm.nih.gov/pubmed/19915566. 764 Cohen MR, Maunsell JHR (2011) Using Neuronal Populations to Study the Mechanisms 765 Underlying Spatial and Feature Attention. Neuron 70:1192–1204 Available at: http://dx.doi.org/10.1016/j.neuron.2011.04.029. 766 767 Compton RJ, Gearinger D, Wild H, Rette D, Heaton EC, Histon S, Thiel P, Jaskir M (2021) 768 Simultaneous EEG and pupillary evidence for post-error arousal during a speeded performance 769 task. Eur J Neurosci 53:543-555 Available at: 770 http://www.ncbi.nlm.nih.gov/pubmed/32854136. 771 Cowley BR, Snyder AC, Acar K, Williamson RC, Yu BM, Smith MA (2020) Slow Drift of Neural 772 Activity as a Signature of Impulsivity in Macaque Visual and Prefrontal Cortex. Neuron 773 108:551-567.e8 Available at: https://doi.org/10.1016/j.neuron.2020.07.021. Crapse TB, Lau H, Basso MA (2018) A Role for the Superior Colliculus in Decision Criteria. 774 775 Neuron 97:181-194.e6 Available at: https://doi.org/10.1016/j.neuron.2017.12.006. 776 Cunningham JP, Yu BM (2014) Dimensionality reduction for large-scale neural recordings. Nat 777 Neurosci 17:1500-1509.
- de Gee JW, Colizoli O, Kloosterman NA, Knapen T, Nieuwenhuis S, Donner TH (2017) Dynamic modulation of decision biases by brainstem arousal systems. Elife 6:1–36 Available at:
- 780 http://www.ncbi.nlm.nih.gov/pubmed/28383284.
- Del Cul A, Baillet S, Dehaene S (2007) Brain dynamics underlying the nonlinear threshold for access to consciousness. PLoS Biol 5:2408–2423.
- Desimone R, Schein SJ (1987) Visual properties of neurons in area V4 of the macaque: Sensitivity

- 784 to stimulus form. J Neurophysiol 57:835–868.
- 785 Di Stasi LL, Catena A, Cañas JJ, Macknik SL, Martinez-Conde S (2013) Saccadic velocity as an
- arousal index in naturalistic tasks. Neurosci Biobehav Rev 37:968–975.
- 787 Diamond MR, Ross J, Morrone MC (2000) Extraretinal control of saccadic suppression. J Neurosci
- 788 20:3449–3455 Available at: http://www.ncbi.nlm.nih.gov/pubmed/10777808.
- 789 DiGirolamo GJ, Patel N, Blaukopf CL (2016) Arousal facilitates involuntary eye movements. Exp
- 790 Brain Res 234:1967–1976.
- 791 Dimigen O, Valsecchi M, Sommer W, Kliegl R (2009) Human microsaccade-related visual brain
- 792 responses. J Neurosci 29:12321–12331.
- 793 Donoghue T, Haller M, Peterson EJ, Varma P, Sebastian P, Gao R, Noto T, Lara AH, Wallis JD,
- Knight RT, Shestyuk A, Voytek B (2020) Parameterizing neural power spectra into periodic
- and aperiodic components. Nat Neurosci 23:1655–1665 Available at:
- 796 http://dx.doi.org/10.1038/s41593-020-00744-x.
- 797 Donoghue T, Schaworonkow N, Voytek B (2021) Methodological considerations for studying
- 798 neural oscillations. Eur J Neurosci:1–26.
- 799 Driscoll LN, Pettit NL, Minderer M, Chettih SN, Harvey CD (2017) Dynamic Reorganization of
- Neuronal Activity Patterns in Parietal Cortex. Cell 170:986-999.e16.
- 801 Engbert R, Kliegl R (2003) Microsaccades uncover the orientation of covert attention. Vision Res
- 802 43:1035–1045.
- 803 Ergenoglu T, Demiralp T, Bayraktaroglu Z, Ergen M, Beydagi H, Uresin Y (2004) Alpha rhythm of
- the EEG modulates visual detection performance in humans. Brain Res Cogn Brain Res
- 20:376–383 Available at: http://www.ncbi.nlm.nih.gov/pubmed/15268915.
- Foote SL, Aston-Jones G, Bloom FE (1980) Impulse activity of locus coeruleus neurons in awake
- rats and monkeys is a function of sensory stimulation and arousal. Proc Natl Acad Sci U S A
- 808 77:3033–3037.
- Fuster JM, Alexander GE (1971) Neuron activity related to short-term memory. Science 173:652–

810	654 Available at: http://www.ncbi.nlm.nih.gov/pubmed/4998337.
811	Green DM, Swets JA (1966) Signal detection theory and psychophysics. Wiley.
812	Hafed ZM (2013) Alteration of Visual Perception prior to Microsaccades. Neuron 77:775–786
813	Available at: http://dx.doi.org/10.1016/j.neuron.2012.12.014.
814	Hafed ZM, Ignashchenkova A (2013) On the Dissociation between Microsaccade Rate and
815	Direction after Peripheral Cues: Microsaccadic Inhibition Revisited. J Neurosci 33:16220-
816	16235.
817	Hafed ZM, Krauzlis RJ (2010) Microsaccadic suppression of visual bursts in the primate superior
818	colliculus. J Neurosci 30:9542–9547 Available at:
819	http://www.ncbi.nlm.nih.gov/pubmed/20631182.
820	Hanslmayr S, Aslan A, Staudigl T, Klimesch W, Herrmann CS, Bäuml K-H (2007) Prestimulus
821	oscillations predict visual perception performance between and within subjects. Neuroimage
822	37:1465–1473 Available at: http://www.ncbi.nlm.nih.gov/pubmed/16971533.
823	Harris KD (2020) Nonsense correlations in neuroscience. bioRxiv:2020.11.29.402719 Available at:
824	https://doi.org/10.1101/2020.11.29.402719.
825	Harvey CD, Coen P, Tank DW (2012) Choice-specific sequences in parietal cortex during a virtual-
826	navigation decision task. Nature 484:62-68 Available at:
827	http://www.ncbi.nlm.nih.gov/pubmed/22419153.
828	Hennig JA, Oby ER, Golub MD, Bahureksa LA, Sadtler PT, Quick KM, Ryu SI, Tyler-Kabara EC,
829	Batista AP, Chase SM, Yu BM (2021) Learning is shaped by abrupt changes in neural
830	engagement. Nat Neurosci 24:727-736 Available at: http://dx.doi.org/10.1038/s41593-021-
831	00822-8.
832	Hong L, Walz JM, Sajda P (2014) Your eyes give you away: Prestimulus changes in pupil diameter
833	correlate with poststimulus task-related EEG dynamics. PLoS One 9.
834	Iemi L, Busch NA, Laudini A, Haegens S, Samaha J, Villringer A, Nikulin V V (2019) Multiple
835	mechanisms link prestimulus neural oscillations to sensory responses. Elife 8:1615–1628

836	Available at: http://www.ncbi.nlm.nih.gov/pubmed/24405187.
837	Iemi L, Chaumon M, Crouzet SM, Busch NA (2017) Spontaneous neural oscillations bias
838	perception by modulating baseline excitability. J Neurosci 37:807-819.
839	Johnston R, Snyder AC, Khanna SB, Issar D, Smith MA (2021) The Eyes Reflect an Internal
840	Cognitive State Hidden in the Population Activity of Cortical Neurons. Cereb Cortex:1-16
841	Available at: http://www.ncbi.nlm.nih.gov/pubmed/34963140.
842	Jolliffe IT, Cadima J (2016) Principal component analysis: a review and recent developments.
843	Philos Trans R Soc A Math Phys Eng Sci 374:20150202 Available at:
844	https://royalsocietypublishing.org/doi/10.1098/rsta.2015.0202.
845	Joshi S, Gold JI (2020) Pupil Size as a Window on Neural Substrates of Cognition. Trends Cogn Sci
846	24:466–480 Available at: https://doi.org/10.1016/j.tics.2020.03.005.
847	Joshi S, Li Y, Kalwani RM, Gold JI (2016) Relationships between Pupil Diameter and Neuronal
848	Activity in the Locus Coeruleus, Colliculi, and Cingulate Cortex. Neuron 89:221-234
849	Available at: http://dx.doi.org/10.1016/j.neuron.2015.11.028.
850	Jun EJ, Bautista AR, Nunez MD, Allen DC, Tak JH, Alvarez E, Basso MA (2021) Causal role for
851	the primate superior colliculus in the computation of evidence for perceptual decisions. Nat
852	Neurosci 24:1121–1131 Available at: http://dx.doi.org/10.1038/s41593-021-00878-6.
853	Kelly RC, Smith MA, Samonds JM, Kohn A, Bonds AB, Movshon JA, Lee TS (2007) Comparison
854	of recordings from microelectrode arrays and single electrodes in the visual cortex. J Neurosci
855	27:261–264 Available at: http://www.ncbi.nlm.nih.gov/pubmed/17215384.
856	Kelly SP, Lalor EC, Reilly RB, Foxe JJ (2006) Increases in alpha oscillatory power reflect an active
857	retinotopic mechanism for distracter suppression during sustained visuospatial attention. J
858	Neurophysiol 95:3844–3851.
859	Khanna SB, Snyder AC, Smith MA (2019) Distinct Sources of Variability Affect Eye Movement
860	Preparation. J Neurosci 39:4511–4526 Available at:
861	http://www.ncbi.nlm.nih.gov/pubmed/30914447.

862	Knöll J, Binda P, Morrone MC, Bremmer F (2011) Spatiotemporal profile of peri-saccadic contrast
863	sensitivity. J Vis 11:1657–1673 Available at: http://www.ncbi.nlm.nih.gov/pubmed/28100659.
864	Leavitt ML, Pieper F, Sachs AJ, Martinez-Trujillo JC (2017) Correlated variability modifies
865	working memory fidelity in primate prefrontal neuronal ensembles. Proc Natl Acad Sci U S A
866	114:E2494–E2503 Available at: http://www.ncbi.nlm.nih.gov/pubmed/28275096.
867	Limbach K, Corballis PM (2016) Prestimulus alpha power influences response criterion in a
868	detection task. Psychophysiology 53:1154–1164.
869	Luck SJ, Woodman GF, Vogel EK (2000) Event-related potential studies of attention. Trends Cogn
870	Sci 4:432–440.
871	Luo TZ, Maunsell JHR (2015) Neuronal Modulations in Visual Cortex Are Associated with Only
872	One of Multiple Components of Attention. Neuron 86:1182–1188 Available at:
873	http://dx.doi.org/10.1016/j.neuron.2015.05.007.
874	Luo TZ, Maunsell JHR (2018) Attentional Changes in Either Criterion or Sensitivity Are Associated
875	with Robust Modulations in Lateral Prefrontal Cortex. Neuron 97:1382-1393.e7 Available at:
876	https://doi.org/10.1016/j.neuron.2018.02.007.
877	Mangun GR, Hillyard SA (1991) Modulations of Sensory-Evoked Brain Potentials Indicate
878	Changes in Perceptual Processing During Visual-Spatial Priming. J Exp Psychol Hum Percept
879	Perform 17:1057–1074.
880	Mante V, Sussillo D, Shenoy K V., Newsome WT (2013) Context-dependent computation by
881	recurrent dynamics in prefrontal cortex. Nature 503:78-84 Available at:
882	http://www.ncbi.nlm.nih.gov/pubmed/24201281.
883	Martinez-Conde S, Otero-Millan J, MacKnik SL (2013) The impact of microsaccades on vision:
884	Towards a unified theory of saccadic function. Nat Rev Neurosci 14:83-96.
885	Mathewson KE, Gratton G, Fabiani M, Beck DM, Ro T (2009) To see or not to see: prestimulus
886	alpha phase predicts visual awareness. J Neurosci 29:2725–2732 Available at:
887	http://www.ncbi.nlm.nih.gov/pubmed/19261866.

888	Mierau A, Klimesch W, Lefebvre J (2017) State-dependent alpha peak frequency shifts:
889	Experimental evidence, potential mechanisms and functional implications. Neuroscience
890	360:146–154.
891	Moran J, Desimone R (1985) Selective attention gates visual processing in the extrastriate cortex.
892	Science 229:782-784 Available at: https://www.science.org/doi/10.1126/science.4023713.
893	Murray JD, Bernacchia A, Roy NA, Constantinidis C, Romo R, Wang X-J (2017) Stable population
894	coding for working memory coexists with heterogeneous neural dynamics in prefrontal cortex.
895	Proc Natl Acad Sci U S A 114:394–399 Available at:
896	http://www.ncbi.nlm.nih.gov/pubmed/28028221.
897	Musall S, Kaufman MT, Juavinett AL, Gluf S, Churchland AK (2019) Single-trial neural dynamics
898	are dominated by richly varied movements. Nat Neurosci 22:1677-1686 Available at:
899	http://dx.doi.org/10.1038/s41593-019-0502-4.
900	Musall S, von Pföstl V, Rauch A, Logothetis NK, Whittingstall K (2014) Effects of neural
901	synchrony on surface EEG. Cereb Cortex 24:1045–1053 Available at:
902	http://www.ncbi.nlm.nih.gov/pubmed/23236202.
903	Ni AM, Ruff DA, Alberts JJ, Symmonds J, Cohen MR (2018) Learning and attention reveal a
904	general relationship between population activity and behavior. Science 359:463-465 Available
905	at: http://www.ncbi.nlm.nih.gov/pubmed/29371470.
906	Oby ER, Golub MD, Hennig JA, Degenhart AD, Tyler-Kabara EC, Yu BM, Chase SM, Batista AP
907	(2019) New neural activity patterns emerge with long-term learning. Proc Natl Acad
908	Sci:201820296 Available at: http://www.pnas.org/lookup/doi/10.1073/pnas.1820296116.
909	Pelli DG (1997) The VideoToolbox software for visual psychophysics: transforming numbers into
910	movies. Spat Vis 10:437-442 Available at: http://www.ncbi.nlm.nih.gov/pubmed/9176953.
911	Peterson EJ, Rosen BQ, Campbell AM, Belger A, Voytek B (2017) 1/F Neural Noise Is a Better
912	Predictor of Schizophrenia Than Neural Oscillations. DoiOrg:113449 Available at:
913	https://www.biorxiv.org/content/early/2017/03/03/113449.

914	Podvalny E, King LE, He BJ (2021) Spectral signature and behavioral consequence of spontaneous
915	shifts of pupil-linked arousal in human. Elife 10:1–25 Available at:
916	http://www.ncbi.nlm.nih.gov/pubmed/34463255.
917	Pourtois G, De Pretto M, Hauert C (2006) Time course of brain activity during change blindness
918	and change awareness: performance J Cogn Neurosci:2108-2129 Available at:
919	http://www.mitpressjournals.org/doi/abs/10.1162/jocn.2006.18.12.2108%5Cnfile:///Users/Meg
920	an/Documents/Papers2/Articles/2006/Pourtois/Time course of brain activity during change
921	blindness and change awareness performance 2006 Pourtois.pdf%5Cnpapers2://pu.
922	Reimer J, McGinley MJ, Liu Y, Rodenkirch C, Wang Q, McCormick DA, Tolias AS (2016) Pupil
923	fluctuations track rapid changes in adrenergic and cholinergic activity in cortex. Nat Commun
924	7:1–7 Available at: http://dx.doi.org/10.1038/ncomms13289.
925	Remington ED, Narain D, Hosseini EA, Jazayeri M (2018) Flexible Sensorimotor Computations
926	through Rapid Reconfiguration of Cortical Dynamics. Neuron 98:1005-1019.e5 Available at:
927	https://doi.org/10.1016/j.neuron.2018.05.020.
928	Roberts DM, Fedota JR, Buzzell GA, Parasuraman R, McDonald CG (2014) Prestimulus
929	oscillations in the alpha band of the EEG are modulated by the difficulty of feature
930	discrimination and predict activation of a sensory discrimination process. J Cogn Neurosci
931	26:1615–1628 Available at: https://www.apa.org/ptsd-
932	guideline/ptsd.pdf%0Ahttps://www.apa.org/about/offices/directorates/guidelines/ptsd.pdf.
933	Robertson MM, Furlong S, Voytek B, Donoghue T, Boettiger CA, Sheridan MA (2019) EEG power
934	spectral slope differs by ADHD status and stimulant medication exposure in early childhood. J
935	Neurophysiol 122:2427–2437.
936	Rolfs M (2009) Microsaccades: Small steps on a long way. Vision Res 49:2415–2441 Available at:
937	http://dx.doi.org/10.1016/j.visres.2009.08.010.
938	Rolfs M, Kliegl R, Engbert R (2008) Toward a model of microsaccade generation: The case of
939	microsaccadic inhibition. J Vis 8:1–23.

940	Romei V, Gross J, Thut G (2010) On the role of prestimulus alpha rhythms over occipito-parietal
941	areas in visual input regulation: correlation or causation? J Neurosci 30:8692-8697 Available
942	at: http://www.ncbi.nlm.nih.gov/pubmed/20573914.
943	Sara SJ (2009) The locus coeruleus and noradrenergic modulation of cognition. Nat Rev Neurosci
944	10:211–223.
945	Sauseng P, Klimesch W, Stadler W, Schabus M, Doppelmayr M, Hanslmayr S, Gruber WR,
946	Birbaumer N (2005) A shift of visual spatial attention is selectively associated with human
947	EEG alpha activity. Eur J Neurosci 22:2917–2926.
948	Scholes C, McGraw P V., Roach NW (2018) Selective modulation of visual sensitivity during
949	fixation. J Neurophysiol 119:2059–2067.
950	Shoham S, Fellows MR, Normann RA (2003) Robust, automatic spike sorting using mixtures of
951	multivariate t-distributions. J Neurosci Methods 127:111–122 Available at:
952	http://www.ncbi.nlm.nih.gov/pubmed/12906941.
953	Smith MA, Sommer MA (2013) Spatial and temporal scales of neuronal correlation in visual area
954	V4. J Neurosci 33:5422–5432 Available at:
955	http://www.jneurosci.org/cgi/doi/10.1523/JNEUROSCI.4782-12.2013.
956	Snyder AC, Foxe JJ (2010) Anticipatory attentional suppression of visual features indexed by
957	oscillatory alpha-band power increases: A high-density electrical mapping study. J Neurosci
958	30:4024–4032.
959	Snyder AC, Issar D, Smith MA (2018a) What does scalp electroencephalogram coherence tell us
960	about long-range cortical networks? Eur J Neurosci 48:2466–2481 Available at:
961	http://www.ncbi.nlm.nih.gov/pubmed/27935037.
962	Snyder AC, Morais MJ, Willis CM, Smith MA (2015) Global network influences on local
963	functional connectivity. Nat Neurosci 18:736–743.
964	Snyder AC, Yu BM, Smith MA (2018b) Distinct population codes for attention in the absence and
965	presence of visual stimulation. Nat Commun 9:4382 Available at:

966	http://www.nature.com/articles/s41467-018-06754-5.
967	Stringer C, Pachitariu M, Steinmetz N, Reddy CB, Carandini M, Harris KD (2019) Spontaneous
968	behaviors drive multidimensional, brainwide activity. Science 364:255 Available at:
969	https://www.sciencemag.org/lookup/doi/10.1126/science.aav7893.
970	Swick D, Pineda JA, Schacher S, Foote SL (1994) Locus coeruleus neuronal activity in awake
971	monkeys: relationship to auditory P300-like potentials and spontaneous EEG. Exp brain Res
972	101:86–92 Available at: http://www.ncbi.nlm.nih.gov/pubmed/7843306.
973	Thut G, Nietzel A, Brandt SA, Pascual-Leone A (2006) Alpha-band electroencephalographic
974	activity over occipital cortex indexes visuospatial attention bias and predicts visual target
975	detection. J Neurosci 26:9494–9502 Available at:
976	http://www.ncbi.nlm.nih.gov/pubmed/16971533.
977	Valente M, Pica G, Bondanelli G, Moroni M, Runyan CA, Morcos AS, Harvey CD, Panzeri S
978	(2021) Correlations enhance the behavioral readout of neural population activity in association
979	cortex. Nat Neurosci 24:975–986 Available at: http://dx.doi.org/10.1038/s41593-021-00845-1.
980	van Dijk H, Schoffelen J-M, Oostenveld R, Jensen O (2008) Prestimulus oscillatory activity in the
981	alpha band predicts visual discrimination ability. J Neurosci 28:1816–1823 Available at:
982	http://www.ncbi.nlm.nih.gov/pubmed/18287498.
983	Van Kempen J, Loughnane GM, Newman DP, Kelly SP, Thiele A, O'Connell RG, Bellgrove MA
984	(2019) Behavioural and neural signatures of perceptual decision-making are modulated by
985	pupil-linked arousal. Elife 8:1–27.
986	Varazzani C, San-Galli A, Gilardeau S, Bouret S (2015) Noradrenaline and dopamine neurons in the
987	reward/effort trade-off: A direct electrophysiological comparison in behaving monkeys. J
988	Neurosci 35:7866–7877.
989	Voytek B, Kramer MA, Case J, Lepage KQ, Tempesta ZR, Knight RT, Gazzaley A (2015) Age-
990	related changes in 1/f neural electrophysiological noise. J Neurosci 35:13257-13265.
991	Worden MS, Foxe JJ, Wang N, Simpson G V. (2000) Anticipatory biasing of visuospatial attention

992	indexed by retinotopically specific alpha-band electroencephalography increases over occipital
993	cortex. J Neurosci 20:1–6.
994	Zohary E, Shadlen MN, Newsome WT (1994) Correlated neuronal discharge rate and its
995	implications for psychophysical performance. Nature 370:140-143 Available at:
996	http://www.ncbi.nlm.nih.gov/pubmed/8022482.
997	Zuber BL, Stark L, Cook G (1965) Microsaccades and the velocity-amplitude relationship for
998	saccadic eye movements. Science 150:1459–1460 Available at:
999	https://www.sciencemag.org/lookup/doi/10.1126/science.150.3702.1459.
1000	